Indian Journal of Engineering & Materials Sciences
Vol. 13, February 2006, pp. 30-36

Perforated plates with a splitter—Unsteady pressure measurements

Subhash C Yaragal

Department of Civil Engineering, National Institute of Technology Karnataka, Surathkal, PO Srinivasnagar 575 025, India

Received 24 August 2004; accepted 7 November 2005

Wind tunnel experiments have been conducted under highly turbulent and disturbed flow conditions over a solid/perforated plate with a long splitter plate in its plane of symmetry. The effect of varied level of perforation of the normal plate on the fluctuating pressures measured across and along the separation bubble has been studied. The distribution of the unsteady surface pressures with variation of the perforation level of the normal plates is also studied. The different perforation levels of the normal plate that is 0%, 10%, 20%, 30%, 40% and 50% are studied. The Reynolds number based on step height is varied from 4×10^3 to 1.2×10^4. It is interesting to note that for 50% perforation of the normal plate, the RMS pressure fluctuation in the flow field gets reduced to around 60% as compared to that for solid normal plate. Analysis of the results show that the maximum fluctuating surface pressures as well as the fluctuating pressures in the flow field can be well correlated.

IPC Code: G01F1/00

Pressure fluctuations are of common occurrence in unsteady fluid flows. Static pressure fluctuations in interior and exterior flows, away from flow boundaries, are important in aero-acoustics. Although not recognized widely, but of great technical significance, is the fact that pressure fluctuations away from flow boundaries can differ substantially from wall measured values. A need to measure these has been long recognized, with reference to aerodynamic applications like jet noise and aircraft cabin noise. A knowledge of pressure fluctuation characteristics is essential for understanding complex flows.

Basically, two types of pressure fluctuation measurements in turbulent flows have been attempted in the past, namely, at the surface and within the flow. From two review articles on the subject by Willmarth[1] and George *et al*.[2], one can understand that pressure fluctuation measurements pose experimental difficulties, particularly for measurements within the flow.

Govinda Ram and Arakeri[3], attempted to measure both surface pressure fluctuations and pressure fluctuations within the flow in the region of separation and re-attachment. They used isosceles triangular nose models of different included angle (2θ), in which the fore body becomes a normal plate when 2θ equals 180°. One of their important findings was that except for the 2θ=180° model, the maximum RMS pressure fluctuation levels in the shear layer are almost equal to the maximum surface RMS pressure fluctuation levels. This finding highlights the importance for measurement of pressure fluctuation level in the shear layer for the 2θ=180° model. Recently, Tsai and Yang[4] measured pressure fluctuations in the turbulent wake flow behind a two-dimensional V-gutter by use of static pressure probe like the one used by Govinda Ram and Arakeri[3].

Disturbed flow over a bluff plate with a long splitter plate has received less attention, although it is an attractive case of re-circulating flow. Ruderich and Fernholz[5], have reported a fairly detailed investigation of such a flow configuration using hot wire and pulsed-wire anemometry. Castro and Haque[6] made a comprehensive set of measurements throughout the separated shear layer and compared their data with that of two-dimensional plane mixing layer. Gupta and Ranga Raju[7] have putforth a method for predicting the mean velocity field downstream of solid and porous fences. The aim of this paper is to study experimentally the effect of varying perforation of the normal plate on fluctuating velocities and fluctuating pressures within the separating and re-attaching flows, and to ascertain the possible correlations.

Experimental Set-up and Methods

Facility

The facility used for the present experimental study is a suction-type low-speed wind tunnel driven by a

E-mail: subhashyaragal@yahoo.com, yaragal@nitk.ac.in

four-bladed fan connected to a 15 HP slip-ring induction motor. Speed control of the 15 HP slip-ring induction motor over a wide range is achieved by using a combination of stator voltage control and rotor resistance control. The cross-sectional area of the test section is 610 mm × 610 mm and its length is 2100 mm. The tunnel contraction ration is 9:1. Several screens and a honeycomb are provided in the upstream settling chamber with a fine mull cloth cover at the bell mouth entry. A velocity survey in the test section showed that it was uniform within 2% of the centerline velocity except for the boundary layer regions. The centre-line turbulence level (u'_{rms}/U_∞) was measured to be 0.3% within the present experimental velocity range of 5-15 m/s.

Model details

The solid/perforated plate is of steel. The fence height h above the splitter plate (of perspex, 10 mm thick and 650 mm long) is h = 12 mm for all the cases except 50% perforated normal plate, for which it is h = 14 mm. The configuration spanned the tunnel width. The perspex splitter plate has surface pressure tappings of hypodermic needles (0.7 mm inner diameter) every 10 mm centre-to-centre, connected by rubber tubing, details of which are shown in Fig. 1. Suitable number of 3 mm circular holes were drilled in stainless steel plates to result in different level of perforation. Six stainless steel plates having 0%, 10%, 20%, 30%, 40% and 50% perforation levels were used in the present experiments. Table 1 gives the details of the models used in the present study.

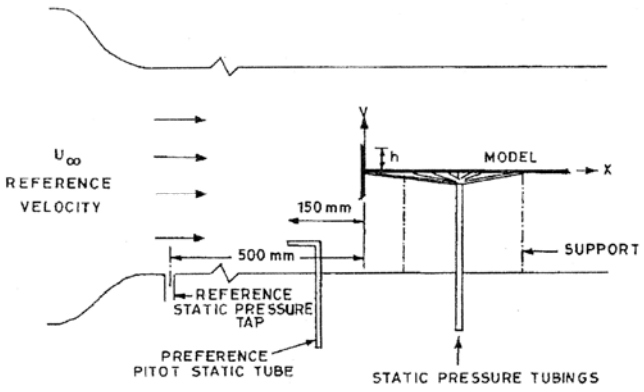

Fig. 1 — Experimental configuration

Flow visualization

Re-attachment length was obtained by a flow-visualization technique. A mixture of titanium oxide, a little oil and soap solution was prepared and a thin coating of this paint was applied on the splitter plate behind the bluff body. Smooth brush and sponge were used for applying the paint evenly on the surface. When the tunnel was started, the mixture moved over the surface, leaving white trails of bigger accumulation indicating the reattachment region. The location of the reattachment point behind the obstructions was in this way found to be within an uncertainty of 5 mm. The reattachment point thus obtained is denoted as X_R.

Fluctuating pressure measurements

Experiments of Kiya and Sasaki[8] have shown that the surface pressure fluctuation can be measured by placing the static pressure probe 1 mm from the surface. A similar arrangement was used in the present measurements. A few preliminary investigations carried out agree well with the measurements of Kiya and Sasaki[8].

The static pressure probe shown in Fig. 2, is a thin round tube 1.3 mm in diameter, bent into an L-shape at a position 37 mm from one end, the other end closed by solder and shaped into a hemispherical form. Four pressure taps 0.5 mm in diameter were drilled onto the tube at a position 9 mm from the hemispherical edge, the other end was directly connected to a Kulite high-sensitive miniature pressure transducer.

Table 1 — Details of the models used in the study

Sl. No	Model	Model notation	Perforation level of the model (%)	Reattachment length (X_R/h)	Aspect ratio	Solid blockage (%)
1	Normal plate/splitter plate combination	NS-0	0	25.2	51	5.6
2	,,	NS-10	10	24.0	51	5.6
3	,,	NS-20	20	23.2	51	5.6
4	,,	NS-30	30	23.2	51	5.6
5	,,	NS-40	40	-	51	5.6
6	,,	NS-50	50	-	44	6.2
7	Right angle corner blunt edge plate	RBP	100	4.8	61	1.6

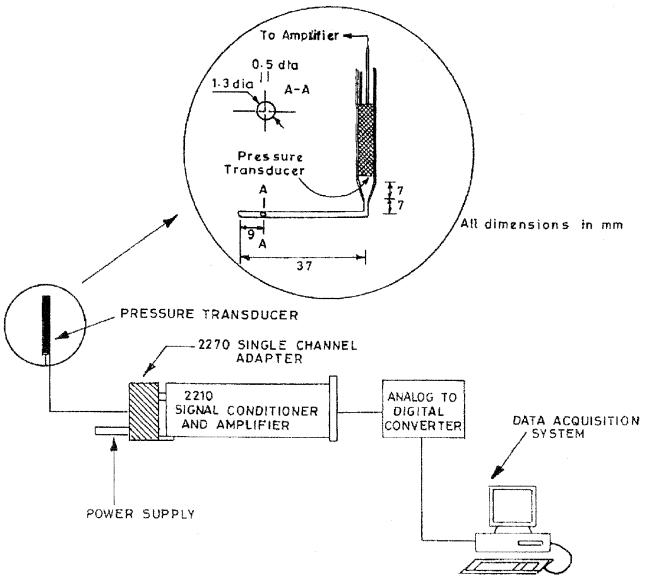

Fig. 2 — Unsteady pressure measurement instrumentation system

Table 2 —Statement of experimental uncertainty

Parameter	Estimated uncertainty	Main source of error
X	±0.5 mm	-
Y, h, D	±0.1 mm	-
X_R	±5 %	Locating the reattachment line from flow visualization studies.
U_∞	±1.5 %	Inaccuracies in reading the height of the meniscus in projection manometer
U'_{rms}	±5 %	Experimental day-to-day repeatability
C_p	±6 %	Inaccuracies in reading from projection manometer and day-to-day repeatability
C'_p	±5 %	Inaccuracy in the dynamic pressure and repeatability of pressure

The pressure transducer used is a silicon sensing diaphragm (Kulite model, Kulite semiconductor products, Inc., Ridgefield, NJ), 2.36 mm in diameter and 50.8 mm long, having high-frequency response and high signal-to-noise ratio. The sensing diaphragm is located below a screen, which protects the transducer from particle contaminants. The amplifier gain was set to provide a sensitivity of 212 Pa/V in the present experiments. The frequency response of the pitot static-pressure probe housing miniature pressure transducer was studied by subjecting to a varied sound-pressure field over a frequency range of 20 Hz-16 kHz. The response of the probe was found to be flat over a frequency range of 125-3000 Hz. Jenkins[9] has studied the effects of enclosing this type of transducer with various tip housings to improve its response for mean and fluctuating pressure measurements.

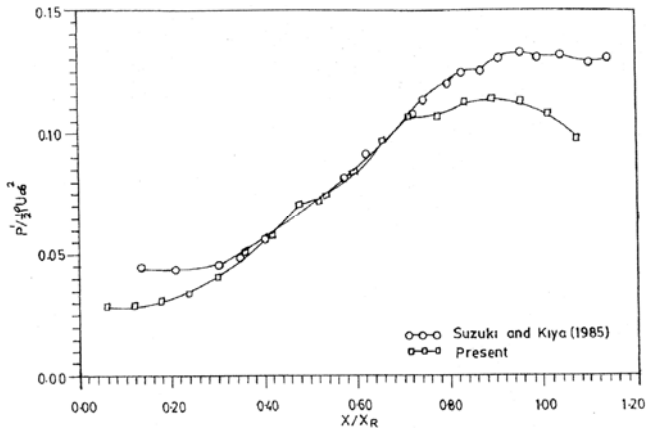

Fig. 3 — Distribution of surface C'_p for solid normal plate compared with results of similar measurements

The output of the pressure transducer was fed to a 2210 signal conditioning amplifier, analogue to digital converter and then to the data acquisition system. Data for each point of pressure measurement consisted of 24000 samples, with the sampling interval of 500 μs. Data were tested at each point for repeatability. The uncertainty of pressure data were found to be less than 5%. Table 2 gives the statement of experimental uncertainty.

Results and Discussion

Fluctuating surface pressure

Suzuki and Kiya[10] have conducted fluctuating surface pressure measurements for isosceles triangular body. The present results of solid normal plate compare well with those of Suzuki and Kiya [for the limiting case of 2θ=180°] as shown in Fig. 3. The experimental result shows similar trend in the curve, that is the RMS values of surface fluctuating pressure increases gradually. It is observed that the maximum RMS values of pressure fluctuation occurs around $0.9\,X_R$, along the plate, and the fluctuating pressures in the separated region is low as compared to the fluctuating pressures across the shear layer. The difference in the C'_p values at $X/X_R = 1$, is attributed to the background noise in measurements. The location of the maximum $C'_{p\,rms}$ upstream of reattachment was observed in several other studies including that of Mabey[11], who considered several geomentries of separated flows. Kiya and Sasaki[12] investigated the separated flow over a blunt flat plate and surmised that the maximum energy associated

Table 3 — Comparison of peak values of RMS fluctuating surface pressures for right angle corner body of different blunt edge thickness

Reference	D^* (mm)	$\left(\frac{X_R}{D}\right)$	$\sqrt{\overline{u'^2}}/U_\infty$ (%)	Reynolds number	$-C_{pb}$	$\sqrt{\overline{p'^2}}/q$ (%)
Hiller & Cherry[13]	38.1	4.88	0.1	3.4 to 8×10^4	0.75	13
Kiya & Sasaki[14]	20	4.7	0.3	2.6×10^4	0.65	15
Present results	10	4.8	0.3	0.4 to 1.2×10^4	0.65	12

* Thickness of the right-angle corner model nose

with the pressure fluctuations near the reattachment region was due to the shedding of large scale vortices from the separation bubble.

Table 3 shows comparison of peak values of fluctuating surface pressures for right-angle corner body with other similar investigations. The body thickness D, the non-dimensional reattachment length X_R/D, upstream turbulence level $(\%)$, Reynolds number based on the body thickness, pressure coefficient C_{pb} at separation and maximum pressure fluctuation are all tabulated.

RMS value of fluctuating surface pressures normalized with dynamic pressure are plotted against x/h for various levels of perforation in Fig. 4. The fluctuating surface pressure distribution trend for all cases considered except the 50% perforated normal plate is the same, that is pressure fluctuations increase from the point of separation and reach a maximum around the reattachment region. The fluctuating surface pressure distribution for 50% perforated normal plate seems to be oscillatory in nature with a local hump in pressure distribution. There is orderly decrease in maximum fluctuating surface pressure with increase in level of perforation of the normal plate. However for the case of 40% perforation, the maximum fluctuating surface pressure happens to be more than that for 30% and 50% perforated normal plates. This could possibly be due to some sort of far wake instability. It is likely that at 40% perforation level the bleed air is just sufficient to introduce instability to the separated shear layer making it unstable and possibly starts to 'flap'. Eventually the flow field pressure fluctuations could be observed to be higher.

The point of maximum surface pressure fluctuation is farthest from the separation point for the solid normal plate and progressively gets closer to the separation point with increase in perforation level. There is a 4.5 step height shift if we compare 0% and 50% perforated normal plate maximum fluctuating surface pressure values. The maximum fluctuating

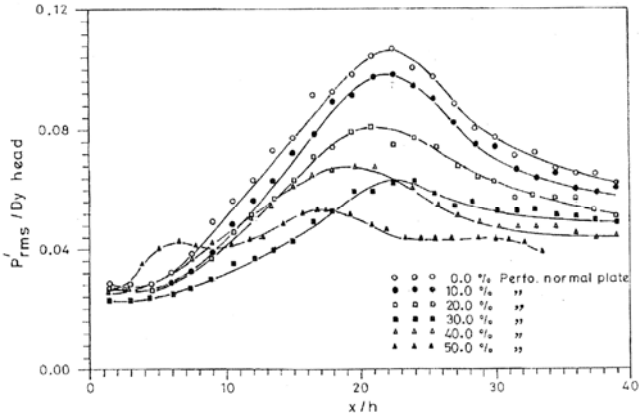

Fig. 4 — Distribution of surface C'_p for various levels of perforation

surface pressure is 11.5% of the dynamic pressure corresponding to the case of solid normal plate and is 5.25% of the dynamic pressure corresponding to 50% perforated normal plate.

The fluctuating surface pressures normalized with dynamic pressure are plotted for higher values of x/h in Fig. 4 to study the effect further downstream of reattachment for varied level of peroration. It is observed that for all cases downstream of reattachment the fluctuating surface pressure is seen to decrease asymptotically. It is interesting to note that in the case of 40% perforated normal plate after reattachment, fluctuating surface pressure value is less than that of 30% perforated normal plate, that is to say recovered fluctuating surface pressures are in order.

Shear layer pressure fluctuation

In the present study the shear layer static pressure fluctuation levels is measured by traversing the static pressure probe across the shear layer at fixed axial location of $x/h = 3, 6, 9, 12, 15, 18, 21, 24, 26$ and 28. The experiments were carried out for three free-stream velocities, viz., 10.0 m/s, 12.5 m/s and 15.0 m/s, to study the speed effects. It is found that the shear layer pressure are independent of Reynolds number in the study range.

Normalized RMS values of pressure fluctuation in the separated bubble region, is shown in Fig. 5. This figure gives the overall qualitative and quantitative picture of the development of shear layer subsequent to separation. The maximum value of shear layer pressure fluctuation is reached upstream of reattachment at an axial location of x equal to about 0.76 X_B. This is in contrast to the observed location of maximum surface pressure fluctuation levels which occurs at $X/X_R = 0.9$. Next possible peak was near the separation point. This peak value may not be only due to the pressure fluctuation, since the pressure measurements were carried out with a finite size transducer probe which leads to spatial averaging of the signal, in addition to unknown interaction of the probe in very thin shear layer at the separation. It was also found for small angles of attack of the probe tube, in the order of ±5 degrees, there was no appreciable change in the readings. Downstream of separation, as the separated shear layer grows, the probe size becomes comparatively small with respect to the eddy size. Consequently, the error involved in the measurement also reduces considerably.

The comparative magnitudes of pressure fluctuations are presented in Fig. 5 that occur as consequence of varying perforation level. As discussed the maximum value of the shear layer pressure fluctuation is reached upstream of reattachment (when it exists) at an axial location of x equal to about 0.76X_R in the case of 0%, 10%, 20% and 30% perforation. With the increase in the level of perforation the point of maximum RMS pressure fluctuation in the flow field moves closer to the splitter plate in a systematic manner. This is indicative that the shear layer gets altered substantially for varied level of perforation.

However, it is to be noted that maximum RMS levels except for the local maxima immediately downstream of separation were observed at about $X/X_R = 0.7$ to 0.8 for the case of 0%, 10%, 20% and 30% perforation and it is interesting to note that for 50% perforation, the RMS pressure fluctuation in the flow field gets reduced to around 60% as compared to solid normal plate.

It was observed that the distribution of fluctuating surface pressures, for the 40% perforated normal plate

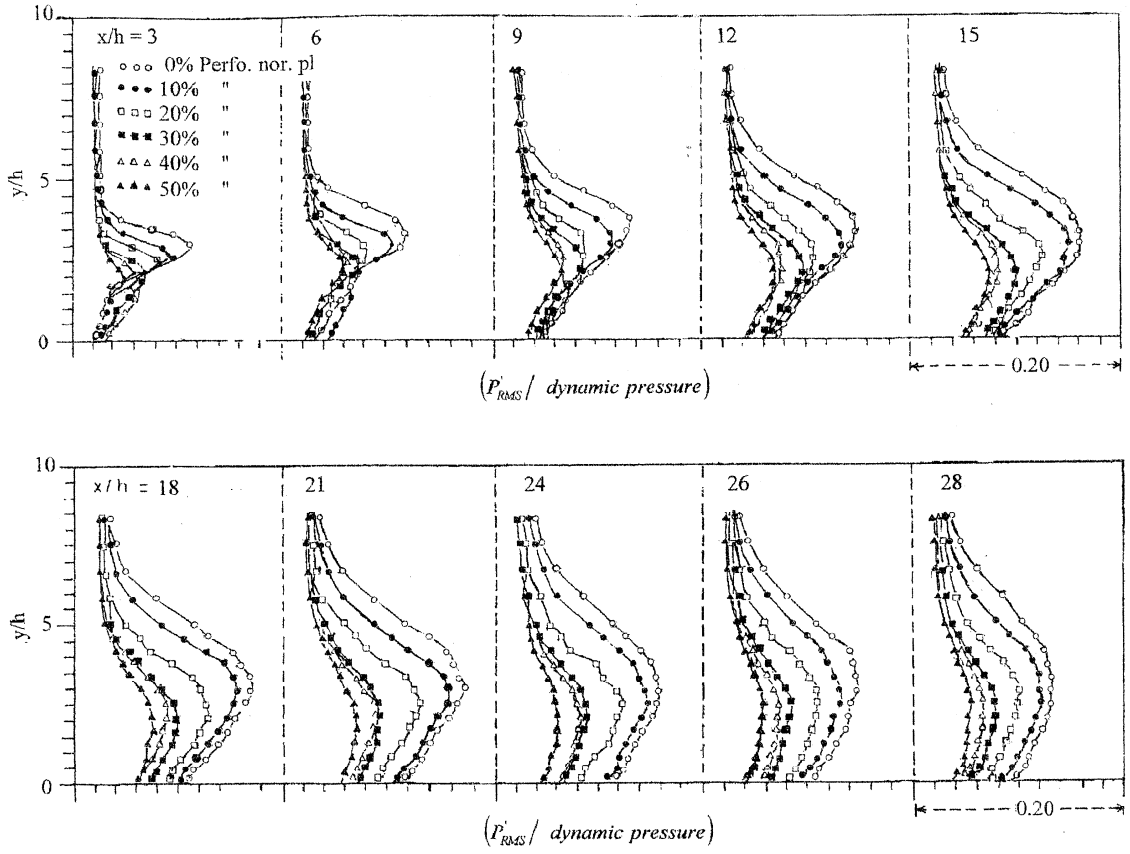

Fig. 5 — The comparative magnitudes of pressure fluctuations in the flow field as a consequence of varying perforation level of the normal plate

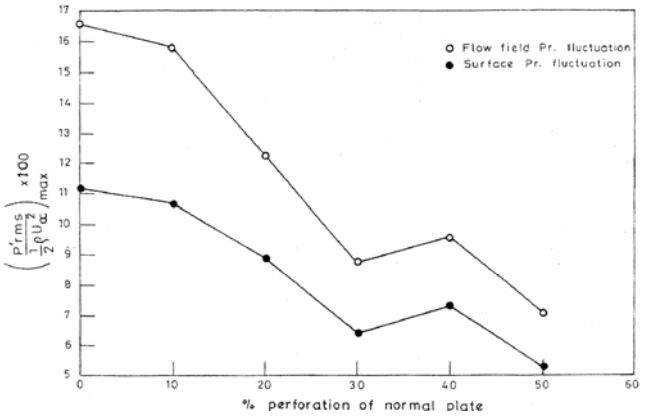

Fig. 6 — Peak RMS values of pressure fluctuation in the separated bubble region and on the surface of the splitter plate for different levels of perforation

was not in order, the same trend is also seen in the distribution of fluctuating pressures in flow field. After $x/h = 18$ the distribution is in order.

In Fig. 6 the magnitude of RMS values of pressure fluctuations measured in the separated shear layer is compared with that obtained in the case of surface pressure fluctuation measurements for varied perforation. It is clear that flow field fluctuating pressures are substantially higher than the surface pressure fluctuations for the cases considered in the present study. As discussed earlier both the surface and flow field fluctuating pressures decrease with increase in the level of perforation. The difference between the surface and flow field maximum pressure fluctuations is highest for solid normal plate (5.4%) and lowest for 50% perforation of the normal plate (2.8%).

It is observed from Table 4, that $\left[\frac{C_p' \text{ max}}{-C_{pb}(1-\eta)}\right]$ varies from 0.200 to 0.238. Analysis of the results seems to indicate a correlation between the maximum of normalized surface RMS pressure fluctuation levels with the $C_{pb}(1-\eta)$. Taking into account the uncertainties in the measurements, the ratio $\left[\frac{C_p' \text{ max}}{-C_{pb}(1-\eta)}\right]$ seems to be relatively constant and has a value of around 0.22.

It is observed from Table 5, that $\left[\frac{C_p' \text{ max}}{-C_{pb}(1-\eta)}\right]$ varies from 0.310 to 0.335. Similar analysis of the results indicate a correlation between the maximum of normalized flow field pressure fluctuation levels with the $C_{pb}(1-\eta)$ value. Taking into account the uncertainties in measurements, this ration seems to be constant and has a value about 0.32.

Table 4 — Ratios of maximum fluctuating surface RMS pressure levels to base pressure coefficient

Sl. No	Model notation	$C_P^{'}$ max	$-C_{Pb}$	$\left[\frac{C_p' \text{ max}}{-C_{pb}(1-\eta)}\right]$
1	NS-0	0.109	0.540	0.200
2	NS-10	0.106	0.533	0.220
3	NS-20	0.081	0.495	0.205
4	NS-30	0.060	0.370	0.231
5	NS-40	0.064	0.485	0.220
6	NS-50	0.050	0.420	0.238

Table 5 — Ratios of maximum fluctuating flow field RMS pressure levels to base pressure coefficient

Sl. No	Model notation	$C_P^{'}$ max	$-C_{Pb}$	$\left[\frac{C_p' \text{ max}}{-C_{pb}(1-\eta)}\right]$
1	NS-0	0.168	0.540	0.311
2	NS-10	0.154	0.533	0.321
3	NS-20	0.123	0.495	0.310
4	NS-30	0.087	0.370	0.335
5	NS-40	0.095	0.485	0.327
6	NS-50	0.070	0.420	0.334

Conclusions

There is substantial modification brought about in the pressure fields as a consequence of change in perforation level of the normal plate, apart from the characteristics of the approach flow itself. It is interesting to note that for 50% perforation, the RMS pressure fluctuation in the flow field gets reduced to around 61.5% as compared to that of the solid normal plate. Analysis of the results show that the ratio $\left[\frac{C_p^{'} \text{ max}}{-C_{pb}(1-\eta)}\right]$ for surface RMS pressure fluctuation levels seems to be constant and has value of about 0.22. Similar analysis show that the ratio $\left[\frac{C_p^{'} \text{ max}}{-C_{pb}(1-\eta)}\right]$ for flow field RMS pressure fluctuation levels seems to be constant and has a value of about 0.32.

Nomenclature

C_{pb} = base pressure coefficient, $\left(P_b - P_\infty\right)/0.5\rho U_\infty^2$
C'_p max = maximum fluctuating pressure coefficient
D = width of the two-dimensional body

η = perforation of the normal plate (ratio of open to total area)
h = step height
P_b = mean base static pressure
P_m = free-stream pressure
$\sqrt{\overline{p'^2}}$ = root mean square pressure fluctuation (P'_{rms})
Re_h = Reynolds number based on step height, $U_\infty h/\nu$
T_u = turbulence intensity
Um = free-stream velocity
u' = fluctuating stream-wise velocity component
$\sqrt{\overline{u'^2}}$ = root mean square velocity fluctuation (u'_{rms})
$\sqrt{\overline{u'^2}}/U_\infty$ = up stream turbulence intensity
x = axial distance downstream of shoulder (point of separation)
X_B = reattachment length
y = distance normal to surface of the splitter plate
2θ = included angle of the fore body
ν = kinematic viscosity of the fluid
ρ = density of the fluid

References

1 Willmarth W W, *Ann Rev Fluid Mech*, 7 (1975) 13.
2 George W K, Benther P D & Arndt R E A, *J Fluid Mech,* 148 (1984**)** 155.
3 Govinda Ram H S & Arakeri V H, *J Fluids Eng*, 112 (1990) 402.
4 Tsai G L & Yang J T, *J Fluids Eng*, 115 (1993) 462.
5 Ruderich R & Fernholz H H, *J Fluid Mech,* 163 (1986) 283.
6 Castro I P & Haque A, *J Fluid Mech,* 179 (1987) 439.
7 Gupta V P & Ranga Raju K G, *J Hydro Eng,* 113 (1987) 1264.
8 Kiya M & Sasaki K, *J Fluid Mech,* 154 (1985) 463.
9 Jenkins R C, *AIAA J,* 25 (1987) 889.
10 Suzuki Y & Kiya M, *Bull JSME,* 28 (243) (1985) 1887.
11 Mabey D G, *J Aircraft,* 9 (9) (1972) 642.
12 Kiya M & Sasaki K, *J Fluid Mech,* 137 (1983) 83.
13 Hiller R & Cherry N J, *J Wind Eng Ind Aerodynam,* 8 (1981) 49.
14 Kiya M & Sasaki K, *J Wind Eng Ind Aerodyam,* 14 (1982) 375.